Tribological aspects of dynamic seals with O-rings used in aircraft hydraulic equipment

Ilie NICOLIN*,[1], Bogdan Adrian NICOLIN[1]

*Corresponding author
[1]INCAS – National Institute for Aerospace Research “Elie Carafoli”,
B-dul Iuliu Maniu 220, Bucharest 061126, Romania,
nicolin.ilie@incas.ro*, nicolin.adrian@incas.ro

DOI: 10.13111/2066-8201.2019.11.2.18

Received: 07 March 2019/ Accepted: 20 May 2019/ Published: June 2019

7th International Workshop on Numerical Modelling in Aerospace Sciences "NMAS 2019"
15-16 May 2019, Bucharest, Romania, (held at INCAS, B-dul Iuliu Maniu 220, sector 6)
Section 3 – Modelling of structural problems in aerospace airframes

Abstract: *Depending on the operating parameters, a dynamic sealing system with O-rings can be in different friction modes: dry, limit, mixed or fluid. Modification of the friction mode occurs throughout the operating life, but also in a single working cycle, as a result working parameters variation: variation in speed of the mobile part of the hydraulic equipment from zero (at start and at reversal of the movement sense) to a maximum value, specific to each application; the fluctuation of the viscosity of the hydraulic fluid according to the pressure and the working temperature; variation of the contact pressures between the sealing ring and the sealing surfaces, depending on the pressure and the temperature of the sealed environment.*

Key Words: *tribology, O-ring, radial, dynamic sealing, hydraulic system, aircraft*

1. CRITERIA FOR CHARACTERIZATION OF THE FRICTION REGIME

Experimentally and practically it was found that when an elastomer slips at a certain speed over a rough surface, in the presence of a fluid, elastohydrodynamic bearing forces exist between the surfaces of the two bodies [6, 7, 8, 9], as shown in Fig. 1. Under certain conditions (relative speed, normal load and type of hydraulic fluid) the two surfaces are completely separated and a continuous fluid film with a very low thickness compared to other body dimensions is interposed between them.

In the case of O-rings, the phenomenon occurs similarly. During relative translation movement between the two surfaces, they can be separated in the presence of a hydraulic fluid, forming a convergent annular gap as shown in Fig. 2 [2, 3, 4, 5, 9, 10, 11].

Given that the static pressure distribution is the result of a major radial deformation (from at least 150 ... 200 μm in the 1.78 mm sectional rings, up to 1100 ... 1200 μm in the sectional rings 6.99 mm), the additional deformation generated by the elastohydrodynamic carrier film cannot significantly alter the initial pressure distribution (the experimentally determined fluid film thickness [1, 2, 3, 4, 5, 9, 10, 11] is of 0 ... 10 μm). The relationship between the elastohydrodynamic pressure p(x), the velocity of the mobile part *V*, the dynamic viscosity of the hydraulic fluid η and the thickness *h(x)* of the film is determined by the Reynolds equation [2, 3, 4, 5, 9, 10, 11]:

$$\frac{\mathrm{dp}}{\mathrm{dx}} = 6 \cdot \eta \cdot V \frac{h(x) - h}{h^3(x)} \tag{1}$$

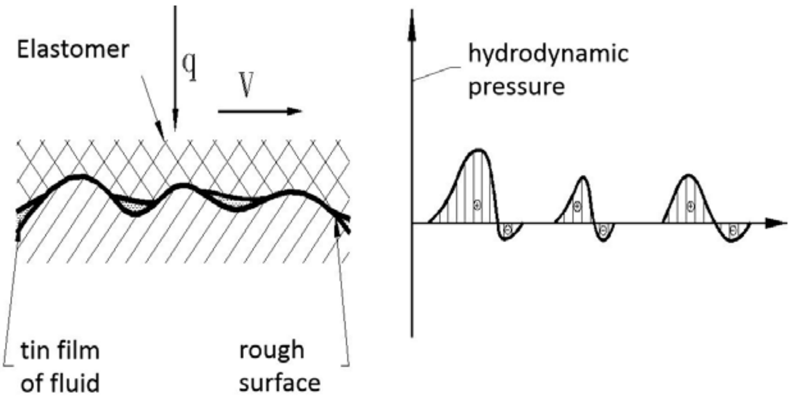

Fig. 1 - Generating hydrodynamic pressure during tangential motion of an elastomeric body over a rigid and rusty surface in the presence of a fluid

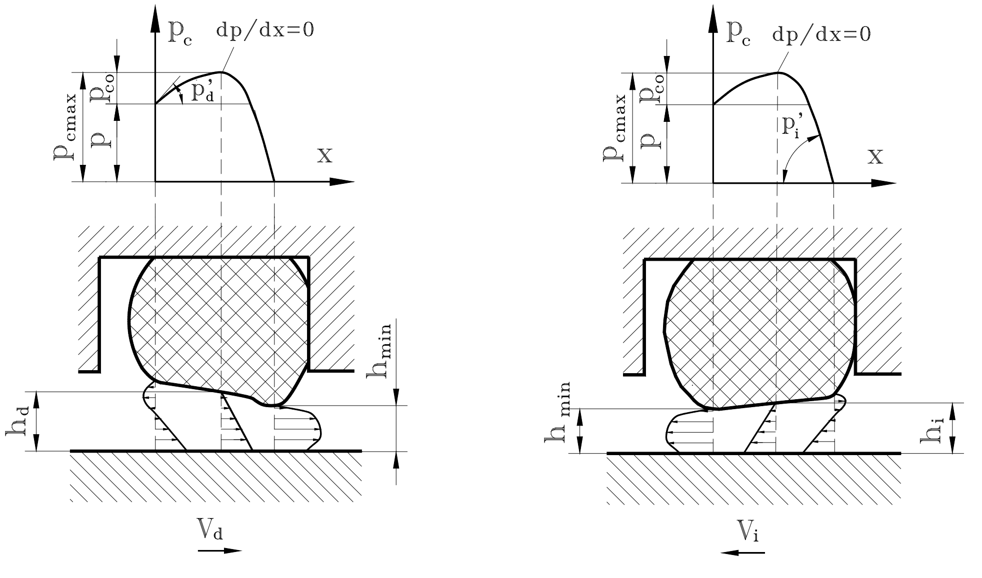

a) direct stroke (the rod comes out of the hydraulic cylinder)

b) reverse stroke (the rod enters the hydraulic cylinder)

Fig. 2 - Diagram of pressure and velocity distribution in the elastohydrodynamic bearing film

in the following calculation hypotheses:

- the elastic pressures generated in the contact area do not change the viscosity of the fluid in the gap;
- the interstice being annular, the lateral flow is negligible;
- the modulus of elasticity of the sealing ring material is very low compared to that of the steel parts;
- the areas of the gap are smooth;

- the thickness of the film is very small compared to other body dimensions and radial grip.

The average thickness of the fluid film h (h_d for the direct stroke or h_i for the reverse stroke), for a known pressure distribution known *p(x)*, analytically or experimentally, corresponds to the point where dp/dx = 0, the elastohydrodynamic pressure value is the maximum and the velocity distribution in the fluid film is linear (from V_d or V_i on the surface of the mobile part to 0 (zero) on the sealing ring surface) and is determined with the following relationships [2, 3, 4, 5, 10, 11]:

$$h_d = \sqrt{\left(\frac{8 \cdot \eta \cdot V_d}{9 \cdot p'_d}\right)} \tag{2}$$

$$h_i = \sqrt{\left(\frac{8 \cdot \eta \cdot V_i}{9 \cdot p'_i}\right)} \tag{3}$$

where p'_d and p'_i are the pressure gradients at the points where the curve has the maximum ascending slope and the maximum descending slope, respectively.

The gradient pressure for direct stroke can be calculated by deriving relationship (4) at point $x = -b'$:

$$p_c(x) = s \cdot p + \frac{k}{d_1}\left(\sqrt{r_*^2 - x^2} - (r_* - \delta_o)\right) \tag{4}$$

Thus, relationship (5) is obtained:

$$p'_d = \frac{k}{d_1}\left(\frac{b'}{\sqrt{r_*^2 - b'^2}}\right) \tag{5}$$

in which all notations have been previously defined or are obtained from experimental pressure variation curves.

For the reverse stroke, the pressure gradient will be calculated with the following relationship:

$$p'_i = p'_d + 0{,}09 \cdot p^{1{,}8} \tag{6}$$

valid for O-ring seals [3, 4], because the gradient calculation by deriving relationship (7) would introduce significant errors in this case, as can be seen from Fig. 4.

The contact pressure distributed on strip $2b$ (see Fig. 3) is calculated with the following relation, for $x \in [-b', b']$:

$$p_c(x) = s \cdot p + \frac{k}{d_1}\left(\sqrt{r_*^2 - x^2} - (r_* - \delta_o)\right) \tag{7}$$

in which:

$$r_* = \frac{b'^2 + \delta_o^2}{2\delta_o} \tag{8}$$

$$\delta_o = \frac{\delta_{\mathrm{ob}} + \delta_{\mathrm{oz}}}{2} \tag{9}$$

and with the below relationship for $x \in (2b', 2b]$:

$$p_c(x) = s \cdot p \cdot \left(\frac{2b - x}{2b - 2b'}\right) \tag{10}$$

The correctness of the calculation relations (7) and (10) was verified by the comparative analysis of the pressure distributions obtained experimentally [3, 4, 10, 11] and analytically, as shown in Fig. 4.

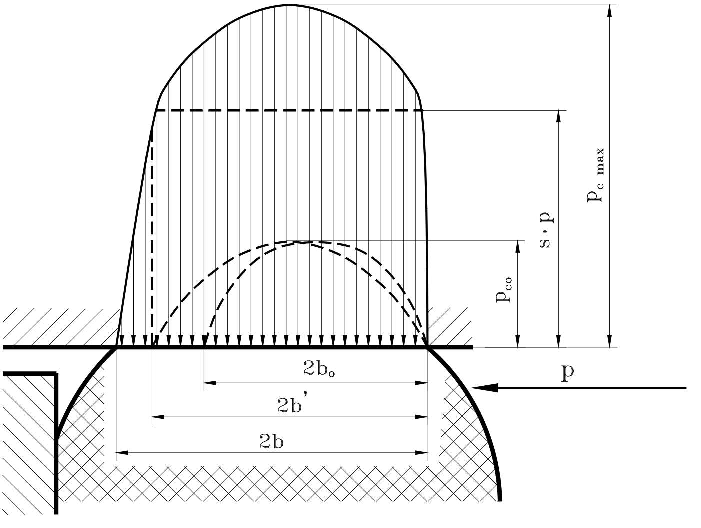

Fig. 3 - Diagram of the contact pressure distribution under pressure from the sealed environment

For the characterization of the friction modes, an adimensional criterion h_r, called the relative thickness of the hydraulic fluid film, defined as the ratio of the thickness of the fluid film to the R_z parameter of the main sealing surface:

$$h_r = h/R_z \tag{11}$$

where h is the thickness of the hydraulic fluid film, and R_z is the average depth (amplitude) of the main sealing surface asperities.

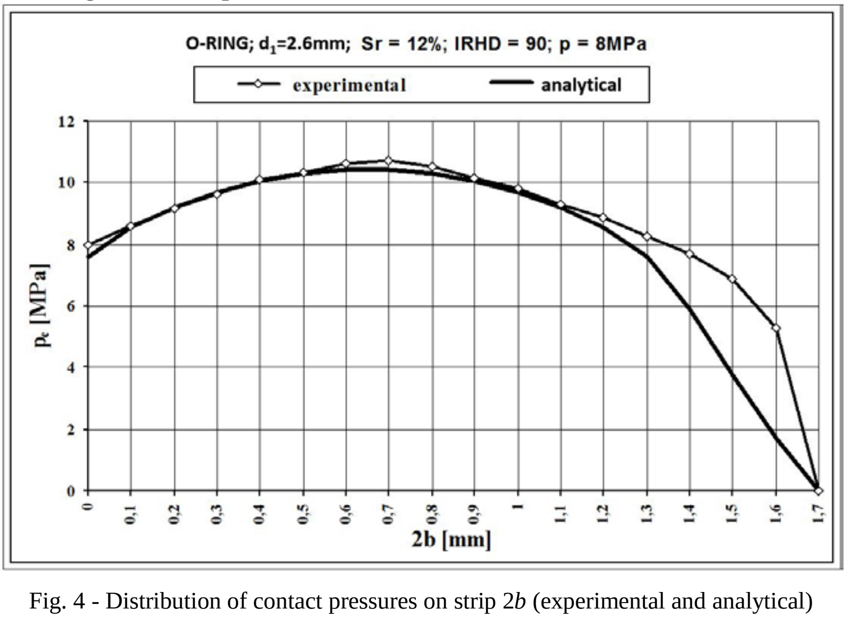

Fig. 4 - Distribution of contact pressures on strip 2*b* (experimental and analytical)

The qualitative dependence of the friction coefficient, according to the value of the dimensionless criterion h_r [3, 4] is shown in Fig. 5, on the basis of which the areas of existence of the friction regimes can be estimated.

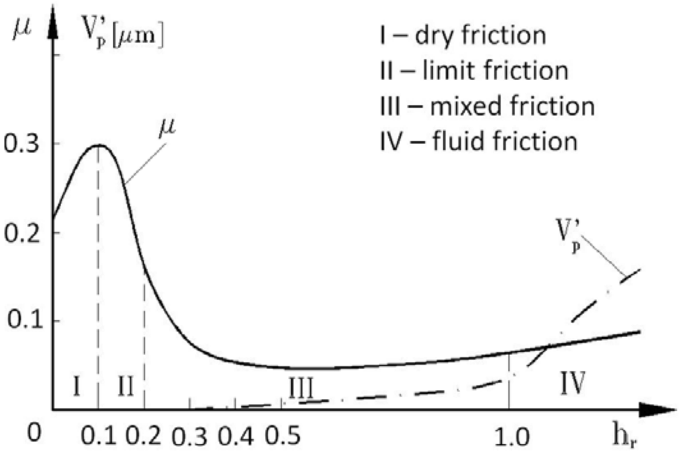

Fig. 5 - Qualitative variation of friction coefficient and relative hydraulic fluid leakage

For low values of the non-dimensional criterion h_r = 0 ... 0.1, the friction mode is considered to be dry; for h_r = 0.1 ... 0.2, the friction mode is considered to be limit; for h_r = 0.2 ... 1.0 the friction mode is considered to be mixed. Naturally, if h > R_z, so h_r > 1, the friction regime becomes fluid.

From relations (2) and (3), if $h_d = R_z$ and $h_i = R_z$, respectively, $h_r = 1$, we can determine the calculation relations for the minimum transition speeds to the V_{tr} friction fluid regime for each movement direction of the mobile part:

$$V_{\mathrm{tr}_d} = \frac{R_z^2}{k_d^2} \cdot \frac{9 \cdot p'_d}{8 \cdot h} \tag{12}$$

$$V_{\mathrm{tr}_i} = \frac{R_z^2}{k_i^2} \cdot \frac{9 \cdot p'_i}{8 \cdot h} \tag{13}$$

in which all notations have been previously defined.

2. CALCULATION OF HYDRAULIC FLUID LEAKAGE ACCORDING TO FRICTION MODE

Due to the variation of the functional parameters (the pressure of the sealing medium, the speed of the mobile part, the temperature in the vicinity of the coupling) within the same working cycle, the average thickness of the fluid film between the sealing ring and the main sealing surface has different values on the two mobile parts: h_d for direct stroke and h_i for reverse stroke, calculated with previously defined relationships.

Due to the fact that the thickness of the fluid film was calculated in the section with the linear velocity distribution (from V_d or V_i on the surface of the mobile part at 0 point on the surface of the sealing ring, (see Fig. 2), it results that the average velocity of the fluid flow will be V_d / 2 and V_i / 2, respectively.

On the other hand, the direction of flow is from the inside to the outside for the direct stroke and from the outside to the inside for the inverse stroke, when a part of the leaked fluid returns to the sealed chamber. Therefore, the volume of hydraulic fluid lost in a working cycle can be calculated with the relation:

$$V_p = \frac{\pi \cdot d_b \cdot L_m}{2}(k_d \cdot h_d - k_i \cdot h_i) \tag{14}$$

in which d_b represents the external diameter of the mobile part, L_m is the length of the travel performed by the moving part, *while* k_d and k_i are constant dependent on the friction regime.

To highlight fluid leakage variation, relative to the non-dimensional h_r criterion (relative thickness of the hydraulic fluid film), the notion of hydraulic fluid loss is used by reporting the leak volume to the friction surface $p \cdot d_b \cdot L_m$:

$$V_p' = \frac{k_d \cdot h_d - k_i \cdot h_i}{2} \tag{15}$$

which allows the representation of its variation with the h_r parameter, as shown in Fig. 5.

3. PARTICULARITIES OF FRICTION AND WEAR OF ELASTOMERS

The friction mode of a mobile seal can be dry (at first start after a longer period of stationary), limit (at reversing the motion direction or at start, if the immobilization time is short), mixed on an extended range of the mobile part speed or the non-dimensional h_r and fluid criterion after the non-dimensional h_r criterion becomes over unity or after the mobile part speed exceeds the V_{tr} value, calculated with relation (12) or (13).

The mixed friction mode is characterized by low friction coefficients and relative hydraulic fluid leakage (see Fig. 5). For these reasons, it is desirable for the mixed friction regime to be predominant within the working cycle of a mobile sealing.

Dry and limit modes inevitably occur during the operation of mobile seals (in the above-mentioned situations) and their analysis will be performed.

The friction fluid regime is characterized by low friction coefficients and low wear, but hydraulic fluid losses are significant. For this reason, in the aeronautical field, the maximum speed of the mobile part is limited to lower values of the transition speeds to the fluid friction regime, precisely to limit the hydraulic fluid loss, which can affect the flight safety of the aircraft. The friction and wear mechanism of the elastomers is closely related to the friction mode and the state of the main sealing surface, as shown in Fig. 6.

The frictional force may generally have three distinct components, but their weight differs depending on certain aspects of a constructive-functional nature:

- the friction force adhesion component has a major share only when the surfaces in contact are smooth, clean (no hydraulic fluid is present and there are no impurities in the gap) and when the relative speed is small, so as is the case with dry and limit friction regimes; even the discontinuous existence of the hydraulic fluid film and the existence of asperities of the main sealing surface drastically reduce this friction force component [6, 7, 8, 9, 13, 14];
- the hysteresis component of the friction force has a major share under the conditions of the mixed friction regime and when the main sealing surface has asperities. In this case, the elastomer is continuously deformed to its “flow” over the rigid roughness of the main sealing surface [6, 7, 8, 9] and the energy dissipates through the mechanism of the hysteresis mechanical losses;
- the furrow component is strongly dependent on the roughness at the tip of the asperity and has a significant weight when the peaks of the asperities are very sharp.

Due to the adverse effects of the fissuring component (rapid damage to the sealing rings), it is eliminated by appropriate technological measures during the finishing operations of the main sealing surfaces (the radius at the peaks of the asperities increases to at least 50μm). For this reason, this component of the friction force will not be called into question.

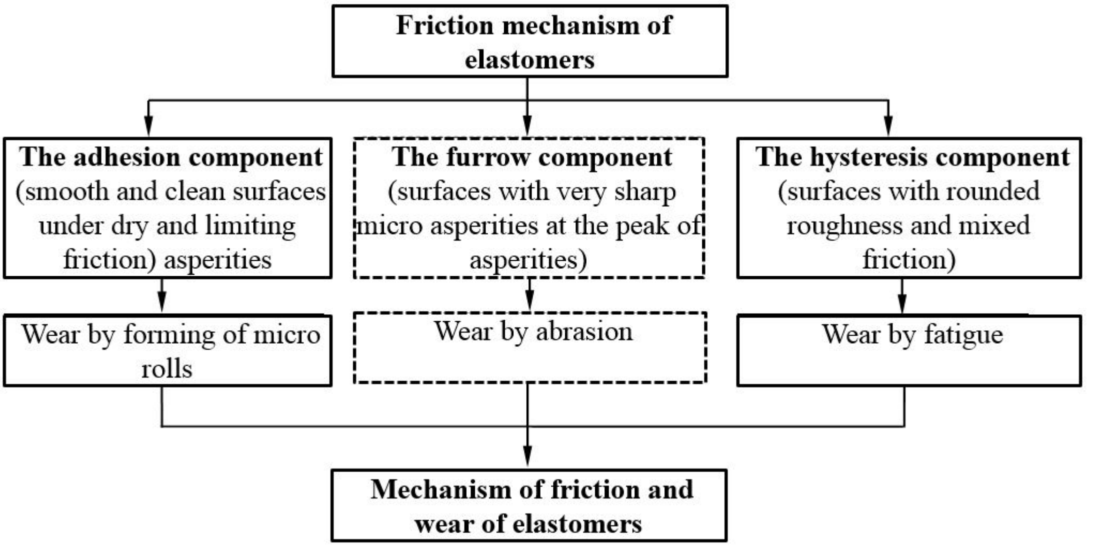

Fig. 6 - Schematic mechanism of friction and wear of elastomers.

The wear mechanism of the elastomers is influenced by the dominant component of the frictional force and the characteristic friction regime.

When the elastomer slides over a rigid, dry or limit surface, the adhesion component is dominant, and this leads to the formation of wear particles called “micro rolls”, similar to those formed when rubbing a school rubber (which is also an elastomer) on the surface of a sheet of paper, the wear being of the adhesive type.

In the mixed mode, the adhesion component is drastically reduced due to the presence of hydraulic fluid at the bottom of the asperities and, inevitably, but in a much lower amount, on both the surface of the elastomer and the tip of the asperities (molecular layers of fluid hydraulic or surface-adsorbed constituents).

Continuous tracking of the contour of the rigid surface by the elastic surface of the elastomer “flowing” over it causes the wear mechanism to be produced by fatigue. As a result, the elastomer surface will crack progressively and wear particles so formed will detach and will be removed during operation [12, 15, 16].

4. CONCLUSIONS

The contact pressure distributed on strip $2b$, for $x \in [-b', b']$ (see Fig. 3) is calculated with (7), respectively (10) for $x \in (2b', 2b]$ (see Fig. 4). The correctness of (7) and (10) was verified by the comparative analysis of the pressure distributions obtained experimentally and analytically, as shown in Fig. 4.

The qualitative dependence of the friction coefficient, according to the value of the dimensionless criterion h_r is shown in Fig. 5, on the basis of which the areas of existence of the friction regimes can be estimated. Relations (12) and (13) allow calculation of minimum transition speeds to the V_{tr} friction fluid regime for each direction of movement of the mobile part. The volume of hydraulic fluid lost is calculated with (15) which allow the representation of its variation with the h_r parameter, as shown in Fig. 5.

The friction and wear mechanism of the elastomers is closely related to the friction mode and the state of the main sealing surface, as shown in Fig. 6.

ACKNOWLEDGEMENT

The work was carried out within the project NUCLEU, contract no. 8N/2019, supported by Romanian Minister of Research and Innovation.

REFERENCES

[1] H. L. Johannesson, Piston rod seal and scraper ring interaction in hydraulic cylinders. Simulation and experiment, *Eurotrib '89*, vol. **4**, p. 139-144, Helsinki, 1989.
[2] A. Karaszkiewicz, (Hydrodynamics or rubber seals for reciprocating motion. Power Int., nr. 389, p. 169-172, 1987). Ghidrodinamica rezinovih uplotnitelinih kolet pri vozvratno-postupatelinom peremesenii, *Express-informatia*, nr. 4 (1989), reference 6, p. 1-9.
[3] L. A. Kondakov, *Uplotnenia i uplotnitelinaia tehnika*, Masinostroenie, Moskva, 1986.
[4] L. A. Kondakov, *Rabocie jidkosti i uplotnenia ghidravliceskih sistem*, Masinostroenie, Moskva, 1982.
[5] C. M. Lang, Elastische Dichtungen-Pressungsverlauf und Reibung. Einfluss von Pressungsgradient, Dichtform und Beans-pruchungsart auf Reibung und Leckverlust, *Maschinenmarkt*, nr. 96, p. 2101-2106, 1969.
[6] D. F. Moore, Friction and wear in rubbers and tires, *Wear*, **61**, p. 273-282, 1980.
[7] D. F. Moore, The tribology of rubberlike materials, *Eurotrib '89*, vol. **3**, p. 288-294, Helsinki, 1989.
[8] D. F. Moore, The elastohydrodinamic transition speed for spheres sliding on lubricated rubber, *Wear*, **35**, p. 159-170, 1975.
[9] D. F. Moore, *Viscoelastic machine elements. Elastomers and lubricants in machine elements*, Butterworth-Heinemann Ltd 1993.
[10] H. K. Müler, Hydrodynamik elastischer Dichtungen, *Oelhydraulik und Pneumatic*, **9**, Nr. 3, p. 89-93, 1965.
[11] H. K. Müler, Leckverluste und Reibung elastischer Dichtungen an hin - und herbewegten Kolbenstangen, *Konstruktion*, **15**, Nr. 4, p. 149-157, 1963.
[12] A. H. Muhr, A. D. Roberts, Rubber abrasion and wear, *Wear*, **158**, p. 213-228, 1992.
[13] A. D. Roberts, A. B. Othman, Rubber adhesion and the dwell time efect, *Wear*, **42**, p. 119-133, 1977.
[14] P. ROUGIER et al., Mechanisms of the sliding wear of rubber, *Wear*, **43**, p. 141-150, 1977.
[15] R. Z. Tudose s.a., *Reologia compusilor macromoleculari*, vol. **1**, **2**, **3**, Editura Tehnica, Bucuresti, 1982.
[16] S. W Zhang, Z. Yang, Energy Theory of Rubber Abrasion by a Line Contact, *Rotrib '96*, Vol. *1*, p. 347-352, Bucuresti.